Structural Evolution and Physical, Optical and Electrochemical Properties of Manganese Ions in Lead Glass

M. Zagrai[1], R.C. Suciu[1], S. Macavei[1], A.Popa[1], S. Rada[1, 2], A. Dehelean[1], and S. Pruneanu[1]

[1]National Institute for Research and Development of Isotopic and Molecular Technologies,400293, Cluj-Napoca, Romania

[2]Physics and Chemistry Department, Technical University of Cluj-Napoca, 400020, Romania

APIM2021 International Conference Processes in Isotopes and Molecules, 22-24 September 2021, Cluj-Napoca, Romania

ABSTRACT Lead glass-ceramics containing transition metal ions are of huge interest because of their electrical and optical properties that makes them suitable for many applications such as electrochemical, electronic, and electro-optic devices. The manganese ion is a highly fascinating ion among different transition metal ions do to the multiple valence states Mn^{2+}, Mn^{3+} and Mn^{4+}. The content of manganese in different valence states depends on the quantitative properties of glass formers and size of the ions in the glass structure. Their simultaneously presence in glass influence on several physical properties of the host glass and makes their electrical properties more interesting. In the present study, lead-manganese glass ceramics was obtained by melt quenching technique and investigated both as alternatives to rare-earth doped luminescent materials and as new electrode materials for lead-acid battery. Characterization techniques including X-ray diffraction (XRD), Cyclic Voltammetry (CV), Fourier Transform Infrared spectroscopy (FT-IR), Ultra Violet-Visible (UV-Vis), Photoluminescence (PL), and Electron Paramagnetic Resonance (EPR) spectroscopy, were used to analyze the compositional dependence of the structural, optical, and electrochemical properties of lead-manganese glass and glass-ceramics.

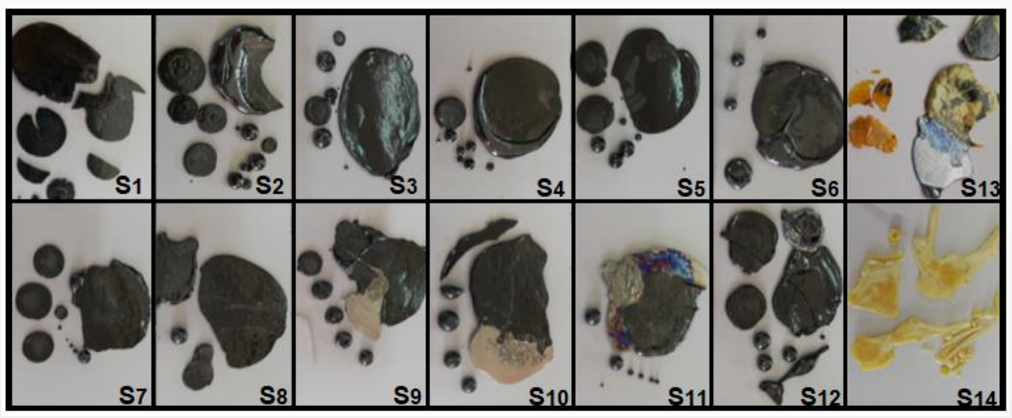

Fig.1: FujiFile images of obtained samples

Experimental procedure

Lead-manganese glasses and glass-ceramics were obtained by melt quenching methods using as starting materials analytical grade reagents PbO_2, MnO_2, and metallic lead powders in stoichiometric amounts *(Figure 1)*. In order to reduce the volatilization of compounds, the weighed batches were melted in alumina crucibles in an electrical oven at 850-950°C, depending on the glass composition. The molten material was pressed and quenched between two stainless-steel plates at room temperature. The CV curves were determined with a typical three-electrode system: the platinum electrode was used as the counter electrode, Ag/AgCl as reference electrode, while S9-S13 samples were employed as working electrodes. The sulfuric acid solution, with a 38% concentration, was used as electrolyte to simulate the electrolyte solution used in the car batteries.

Table 1: The density, optical band gap, and refractive index of samples

Sample	ρ (g/cm³)	E_g (eV)	n
S1	7.270	2.72	2.47
S2	7.046	2.7	2.48
S3	7.210	2.65	2.49
S4	7.250	2.59	2.51
S9	7.306	2.55	2.53
S10	7.082	2.62	2.50
S11	6.806	2.73	2.47
S12	6.316	2.76	2.46
S13	7.029	3.15	2.35
S14	6.812	3.38	2.30

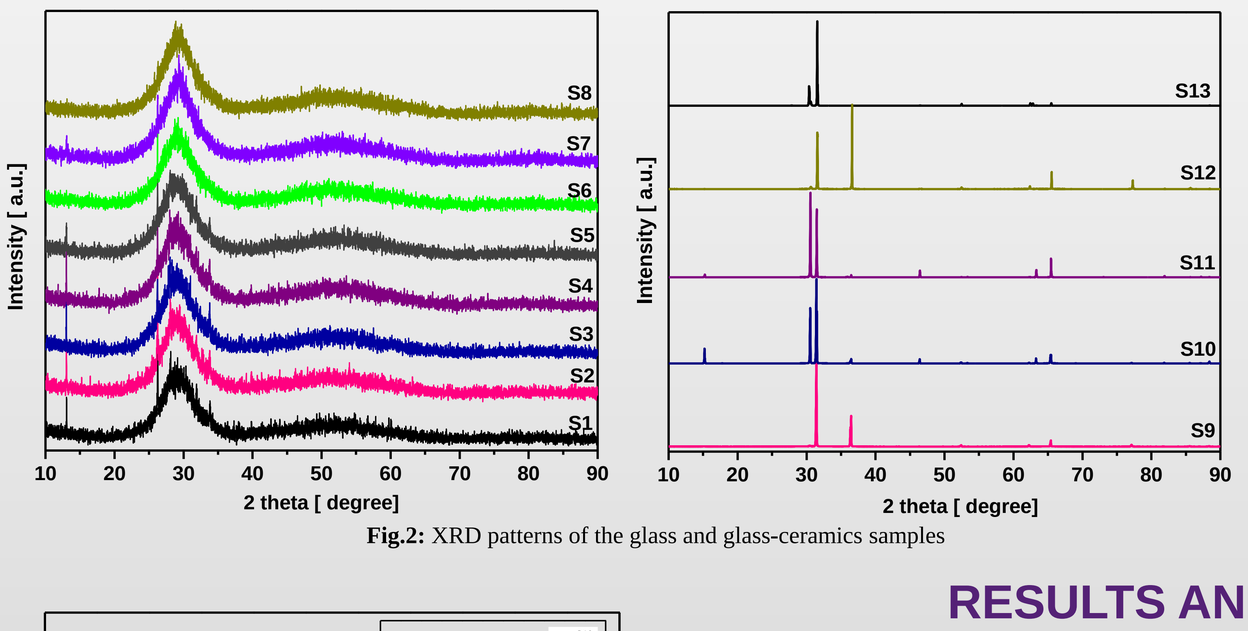

Fig.2: XRD patterns of the glass and glass-ceramics samples

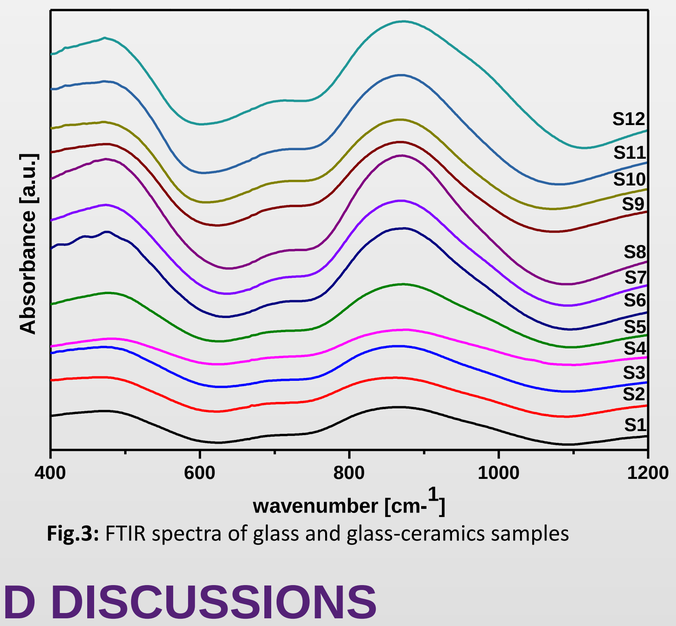

Fig.3: FTIR spectra of glass and glass-ceramics samples

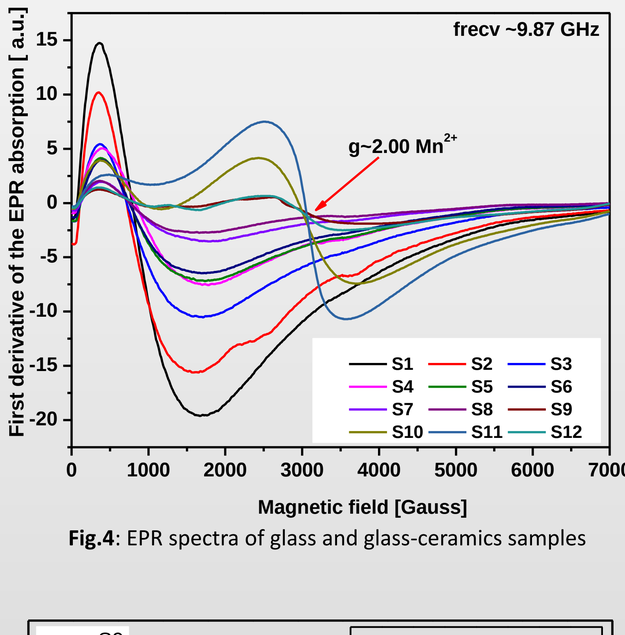

Fig.4: EPR spectra of glass and glass-ceramics samples

RESULTS AND DISCUSSIONS

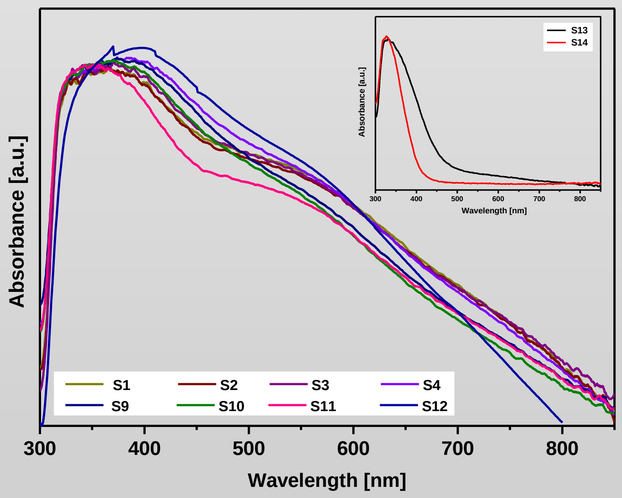

Fig.5: Uv-vis spectra of glass and glass-ceramics samples

The X-ray diffraction data of the studied samples indicate that the S1-S8 samples contain a large amount of amorphous phase and a small quantity of crystalline phase corresponding to $Pb_3Mn_7O_{15}$. Samples S9-S13 have a much better defined crystalline structure. Pb and PbO crystalline phases were identified as the majority phases in these samples. The FTIR spectra show the presence of [PbO_3], [PbO_4], [PbO_6] structural units. The absorption peak around 462 cm^{-1} is related to Pb-O stretching vibration, and the sharp peak around 687 cm^{-1} represents the asymmetric bending vibration of the Pb-O – Pb bond. EPR spectra confirm the presence of the manganese as divalent ion Mn^{2+} in the $3d^5$ electronic configuration. The value of optical band gap energy determined from Ultraviolet-Visible absorption spectra varied from 2.55 to 3.38 eV. The decreasing trends in the optical band gap may be due to the change in the degree of disorder and the number of defects in the glass system.

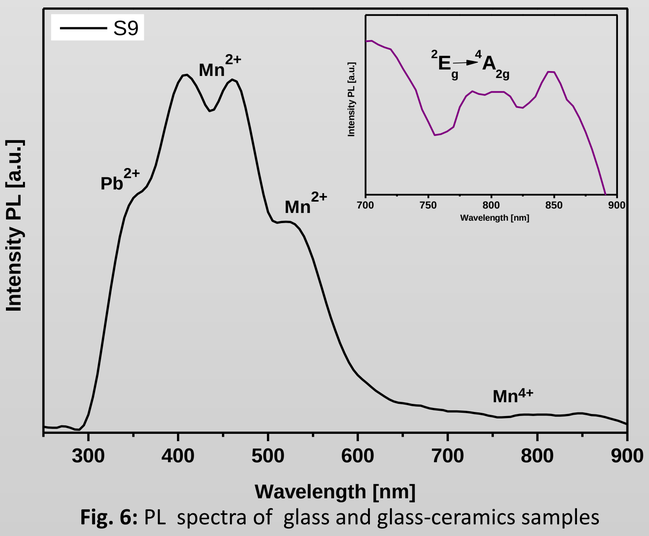

Fig. 6: PL spectra of glass and glass-ceramics samples

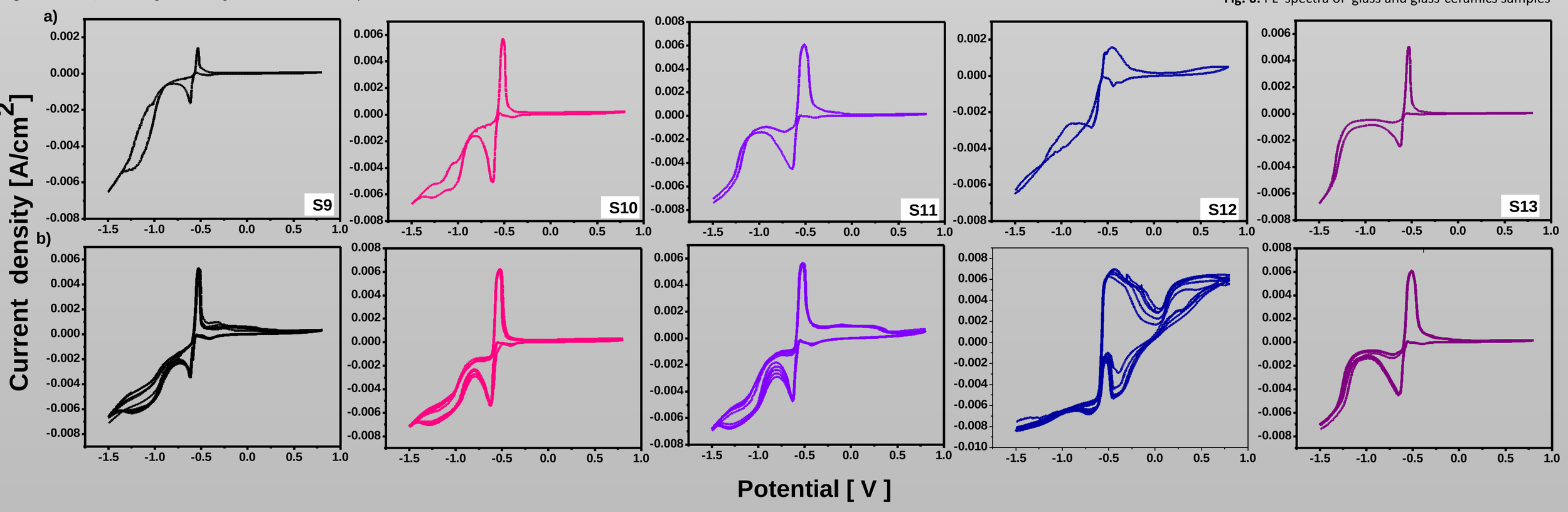

Fig. 7: Cyclic voltammograms of glass-ceramics samples performed between -1.0 V and 1.0 V for one (a) and five (b) cycles with a scan rate of 0.5mV/s in 38% H2SO4 aqueous solution.

The highest refractive index value (2.53) was obtained for the S9 sample due to the high content of non-bridging oxygen. The increase in density is due to the decrease in non-bridging oxygen atoms. Under 200 nm excitation wavelength, the PL spectra show four intensive emission bands in the visible region and five-week emission bands in the near-infrared region, specific to the electronic transitions from the excited states to the ground states of the Pb^{2+}, Mn^{2+} and Mn^{4+} ions. CV was performed on one and five cycles at room temperature, with a scanning speed of 50 mV s^{-1} in a potential range of –1.5 V to +1 V. The cycling voltammograms show good reversibility, after five cycles.

CONCLUSIONS

Structural and behavioral evolution of the vitreous system with MnO2-PbO2-Pb composition, prepared by melt quenching technique, were investigated by X-ray diffraction, FTIR, UV–Vis, PL, and EPR spectroscopy, and Cyclic Voltammetry. Our results reveal outstanding features of the glass-ceramics composition, suitable for optoelectronic applications, and rechargeable batteries.

References: Lemański, K., et. all., J. Mater. Chem. Phys., Vol. 250, 123149, 2020; Dahiya, M. S., et all., J. Non-Cryst. Solids, 485, 24–33, 2018; Zagrai M, et.all., J. Non-Cryst. Solids, 569, 1209881, 2021;

Acknowledgements: This paper was financially supported by the Ministry of Research, Innovation and Digitization: Nucleu-Program, project PN 19 35 01 01 and CNCS/CCCDI – UEFISCDI, project number PN-III-P4-ID-PCCF-2016-0006, within PNCDI III.